SSRG International Journal of Civil Engineering
ISSN: 2348-8352/ https://doi.org/10.14445/23488352/IJCE-V11I4P108

Volume 11 Issue 4, 80-91, April 2024

Original Article

Experimental Investigation of Ferrogeopolymer Confinement for Enhancing Brick Masonry Column Resilience under Axial Compression

R. Jose Antony Syril[1], D. Rajkumar[2]

[1,2]*Department of Civil and Structural Engineering, Annamalai University, Tamilnadu, India.*

[1]*Corresponding Author : joseantonysyrilr@gmail.com*

Received: 15 February 2024 Revised: 27 March 2024 Accepted: 16 April 2024 Published: 30 April 2024

Abstract *- This study investigates the efficacy of ferrogeopolymer confinement in enhancing the resilience of brick masonry columns under axial compression. Previous research has explored various methods of enhancing masonry column resilience, including surface coatings and reinforcement layers. The novelty of the study lies in the utilization of ferrogeopolymer confinement. Fourteen samples are subjected to testing, each featuring different cross-sections and surface coatings (cement mortar and geopolymer mortar) with varying reinforcement layers (single or double-layer welded steel mesh). Results reveal the presence of brittle cracks influenced by mortar type and welded wire mesh reinforcement. Notably, findings demonstrate that geopolymer mortar and welded mesh contribute to improved compressibility, deformation, and load-bearing capabilities compared to unconfined specimens. Moreover, observed higher ductility ratios indicate a more flexible failure mode, particularly noteworthy for structural resilience. Importantly, the study highlights significant variations in energy absorption, with a notable increase observed with double-layer welded mesh, while geopolymer mortar exhibits superior energy absorption. These findings underscore the potential of ferrogeopolymer confinement as a promising strategy for enhancing the resilience of brick masonry columns, offering valuable insights into structural engineering practices.*

Keywords *- Ferrogeopolymer, Masonry columns, Welded mesh, Confinement, Axial Compression.*

1. Introduction

Brick masonry columns have long served as foundational elements in structural engineering, embodying a balance of durability, affordability, and aesthetic appeal [1]. Their historical significance in construction is evident, yet challenges persist in ensuring their resilience, particularly under axial compression [2]. Traditional brick masonry columns, while stalwart in many respects, exhibit limitations in ductility and resistance, particularly under seismic or extreme loading conditions [3]. As seismic events continue to pose significant threats to structures worldwide, an urgent need arises for innovative solutions to fortify brick masonry columns and enhance their performance.

In response to this imperative, researchers and engineers have explored various approaches to augment the resilience of brick masonry columns. Among these strategies, the concept of confinement stands out as a promising avenue for bolstering structural integrity [4–6]. Confinement involves the application of additional materials or techniques to enhance the load-bearing capacity and ductility of structural elements, thereby mitigating the risk of premature failure [6–12]. One such innovative approach gaining traction is the integration of ferrogeopolymer confinement—a composite material comprising geopolymer mortar reinforced with a mesh of closely spaced steel wires or rods [11], [13–17].

Geopolymer-based materials present significant advantages compared to traditional cement-based ones, including enhanced strength, durability, and environmental friendliness [18–20]. A French scientist, Joseph Davidovits, coined the term "geopolymer" to describe alkali aluminosilicate binders formed by activating aluminosilicate materials with alkali silicates. The process of creating these binders involves mixing aluminosilicate precursors like fly ash, metakaolin, or blast furnace slag with alkali activators, typically solutions of alkalis such as sodium hydroxide or potassium hydroxide along with sodium silicate (NaOH or KOH, Na_2SiO_3) [21], [22]. In this study, NaOH and Na_2SiO_3 were used as the activator solution. Incorporating alternative materials not only improves the matrix's properties but also reduces the consumption of natural resources [23–26]. Thus, current research focuses on utilizing fly ash, a byproduct of coal combustion, and manufactured sand (M-sand), an eco-friendly alternative to natural sand, in geopolymer formulations. Fly ash, widely available globally, exhibits

pozzolanic properties suitable for geopolymerization [27], while M-sand offers consistent particle size distribution and superior mechanical properties [28–30]. This incorporation not only reduces reliance on Portland cement but also lessens the environmental impact associated with conventional concrete production. Furthermore, the combination of fly ash and M-sand enhances the workability, strength development, and durability of geopolymer composites synergistically [30].

Research on ferrogeopolymer by various authors underscores its potential to revolutionize construction practices. Studies by Sreevidya et al. (2012, 2014) elucidate the significance of steel mesh layers in enhancing flexural strength and energy absorption in geopolymer ferrocement slabs [31], [32]. Kaliraj et al. (2017) further emphasize the direct correlation between reinforcement volume and energy absorption, particularly in geopolymer ferrocement trough panels [33]. Additionally, Srikrishna and Rao (2020) highlight the comparable mechanical properties between geopolymer and cement mortars, paving the way for sustainable alternatives in construction materials [34].

El-sayed (2021) sheds light on the superior performance of ferrocement geopolymer over traditional steel-reinforced concrete columns, offering promising prospects for cost-effective and eco-friendly structural solutions [14]. Moreover, Sakkarai and Soundarapandian (2021) demonstrate significant improvements in flexural and impact strength with the addition of more wire mesh layers, showcasing the versatility of geopolymer ferrocement in meeting diverse structural demands [35].

On the front of enhancing brick masonry columns with ferrocement, findings from Kibriya (2006) and Shah (2011) underscore its potential to bolster load capacity and crack resistance, thereby enhancing the overall durability of masonry structures [36], [37]. Fossetti and Minafò (2016) contribute valuable insights by comparing different reinforcement methods, with BFRCM jacketing emerging as a promising solution for strength enhancement, particularly in scenarios involving low-grade mortar [38].

Mustafaraj and Yardım (2016) shed light on the ductility and shear strength improvements offered by ferrocement jacketing, affirming its efficacy in enhancing the structural performance of unreinforced masonry walls [39]. Lastly, Sen et al. (2023) delve into the assessment of lateral strength in masonry-infilled RC frames, identifying multiple failure mechanisms and paving the way for further research in optimizing ferrocement applications for seismic retrofitting and strengthening strategies [40]. These collective findings underscore the versatility, durability, and potential applications of ferrocement in enhancing the resilience and longevity of various structural systems.

Based on the literature review, the research gap identified is the lack of investigation into the use of ferrogeopolymer confinement for enhancing the resilience of brick masonry columns under axial compression. While previous studies have explored the effectiveness of ferrocement and geopolymer materials separately, there is limited research on their combined application in masonry column reinforcement. Ferrogeopolymer confinement introduces a novelty by integrating steel reinforcement with geopolymer mortar to enhance the structural performance of brick masonry columns holistically.

The objective of this research involves evaluating the mode of failure and crack patterns in masonry columns with different surface coatings (cement mortar and geopolymer mortar) and additional reinforcement layers (welded steel mesh single-layer and double-layer), assessing axial compression behaviour and deformation, determining ductility compared to traditional reinforcement methods, and measuring energy absorption capacity. Through experimental investigation, the study aims to provide insights into the effectiveness of ferrogeopolymer confinement as a sustainable and resilient reinforcement technique for masonry columns, contributing to advancements in construction practices and structural design.

2. Experimental Investigation

2.1. Materials and Mix Proportion

The materials utilized in this study encompass ordinary Portland cement (grade 53), fine aggregate (manufactured sand), pozzolan (low-calcium Class F fly ash), alkaline activator (sodium hydroxide and sodium silicate), clay burnt bricks, and machine-welded weld mesh with square grid openings. Figure 1 illustrates the materials used in this study.

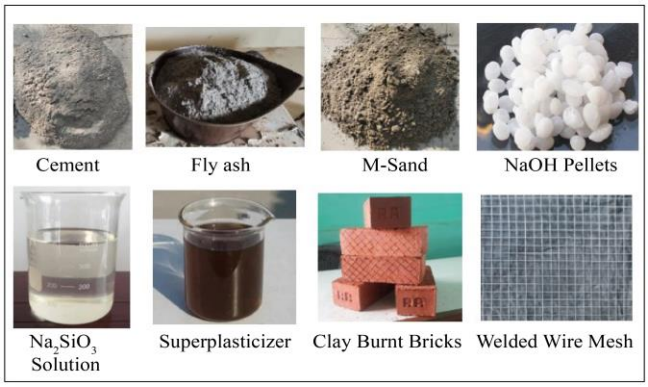

Fig. 1 Materials used

Ordinary Portland cement (53 grade) conforming to IS 12269:1987 [41] sourced from Chettinad Cement for the control mix mortar (CM) and low-calcium Class F fly ash from the Mettur thermal power plant for the geopolymer mix mortar (GPM). Chemical compositions are detailed in Table 1, and physical properties in Table 2. The fine aggregate met

IS 383:2016 standards [42], with specific gravity at 2.80, water absorption at 0.42%, and fineness modulus at 2.90; the grading curve of the fine aggregate is shown in Figure 2.

The addition of Napthalene sulfonate-based superplasticizer (SP) to the binder mass by IS 9103-2018 [43] enhances the effectiveness of mortar. Geopolymer mortar included fly ash, sodium silicates (Na_2SiO_3), sodium hydroxides (NaoH), and distilled water. The activator solution was prepared a day in advance. The mortar mix of binder to fine aggregate ratio is 1:2 and 1:2.5 for conventional and geopolymer. The effectiveness of geopolymer mortar depends on the concentration of sodium hydroxide, which usually falls between 8 to 14 molarity (M) [13, 44, 45]. Generally, an 8M concentration is adequate to achieve the desired strength [45].

In this research, 8M is chosen for the preparation of geopolymer mortar, and the specific mix ratios are provided in the accompanying Table 3, comparing them with conventional mixes. As per IS 4031 (Part 6) - 1988 [46], the mortar cubes of size 70.6mm × 70.6mm × 70.6mm were cast to test the characteristic strength of the mortar mix. The compressive strength of the mortar cubes for conventional and geopolymer are 14.93 N/mm^2 and 21.6 N/mm^2 (average of 10 cubes).

According to IS 1077:1992 [47] non-modular sizes (230mm x 110mm x 70mm), Clay burnt bricks are chosen to construct the brick masonry columns. The bricks had a density of 15.69 kN/mm^2, water absorption of 16.12%, and compressive strength averaging 5.31 N/mm^2. Machine-welded weld mesh had square openings of 20mm × 20mm, with a thickness of 0.75 mm, and ultimate strength values of 465 N/mm^2 as per ASTM A 185 [48].

Table 1. Chemical composition of binders

Component	Cement	Fly Ash
CaO	66.67	1.02
SiO_2	18.91	52.96
Fe_2O_3	4.94	11.02
Al_2O_3	4.51	26.23
SO_3	2.5	1.28
MgO	0.87	0.38
K_2O	0.43	2.82
Na_2O	0.12	0.51
Tio_2	-	2.54
Loss of ignition	1.05	0.52

Table 2. Physical properties of binders

Description	Size	Specific Gravity	Specific Surface Area
Cement	90µ	3.15	290m^2/kg
Fly Ash	10-50µ	2.3	343m^2/kg

Table 3. Mix proportion (kg/m^3)

Description	CM	GPM-8M
Cement	350	-
Fly Ash	-	370.37
Fine aggregate	737.5	781.48
NaoH	-	49.73
Na2SiO3	-	124.33
Water	165	-
SP	1.4	4.4

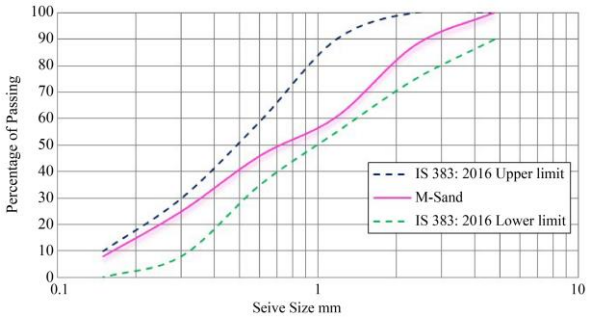

Fig. 2 Grading curve of fine aggregate

2.2. Volume Fraction of Reinforcement

When employing a uniform square or rectangular wire mesh throughout the entire depth of a ferrocement element, the volume fraction of reinforcement can be determined using the equation (1) [13]:

$$V_r = \frac{N\pi d^2_w}{4h}\left[\frac{1}{D_l} + \frac{1}{D_t}\right] \quad (1)$$

In this equation, V_r represents the volume fraction of reinforcement, N denotes the number of mesh layers, π equals approximately 3.14, d^2_w stands for the wire mesh diameter, h indicates the thickness of the Ferrocement element, D_l refers to the center-to-center distance between longitudinal wires, and D_t signifies the center-to-center distance between transverse wires. The calculated volume fraction of confined specimens is displayed in Table 4.

2.3. Specimen Description and Preparation

Fourteen specimens were produced, comprising seven combinations, with two specimens for each combination. Table 4 presents descriptions of the specimens, which are masonry column specimens measuring a constant length of 1200 mm. The varying cross-sections of the individual specimens are detailed in Table 4. The preparation process involved mixing mortar according to prescribed mix proportions, constructing masonry columns using clay burnt bricks, applying surface coatings where applicable, and installing welded wire mesh reinforcement to enhance confinement. Conventional specimens underwent water curing, while geopolymer specimens were subjected to ambient curing conditions. After curing, the specimens were white-washed, dimensionally marked, and transported to the test floor for axial compression testing. The geometry of the unconfined masonry column is shown in Figure 3, and the experimental preparation of specimens is shown in Figure 4.

Table 4. Details of tested specimens

Series	Sample ID	Cross Section	No. of Layers	Volume Fraction %	Sample Description
Conventional	UC	230mm x 230mm	-	-	Specimen without additional confinement material
Conventional Confined	CC-0	250mm x 250mm	-	-	Cement mortar surface coating
	CC-1	270mm x 270mm	1	0.11	Cement mortar with welded mesh single-layer
	CC-2	280mm x 280mm	2	0.18	Cement mortar with welded mesh Double-layer
Geopolymer Confined	GP-0	250mm x 250mm	-	-	Geopolymer mortar surface coating
	GP-1	270mm x 270mm	1	0.11	Geopolymer mortar with welded mesh single-layer
	GP-2	280mm x 280mm	2	0.18	Geopolymer mortar with welded mesh Double-layer

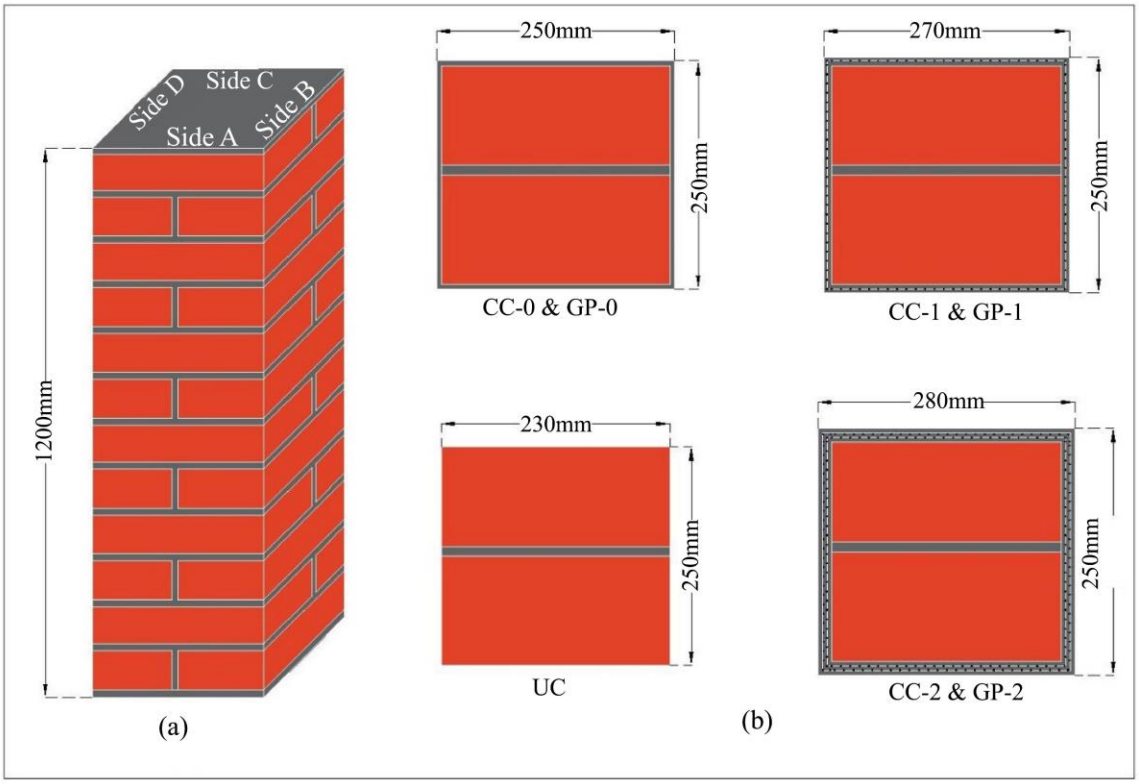

Fig. 3 Geometry of the masonry column (a) Elevation, AND (b) Cross-section.

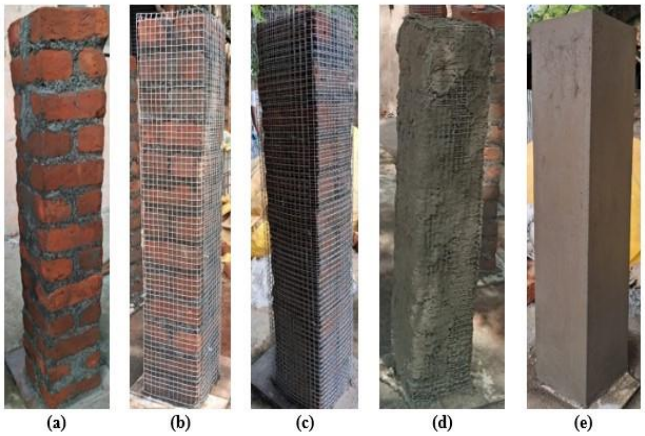

Fig. 4 Preparation of specimens (a) Unconfined, (b) Single layer, (c) Double layer, (d) Applying surface coating, and (e) Surface finished.

2.3. Test Setup

The experimental testing was conducted using a hydraulic testing machine with a maximum capacity of 500 kN, ensuring adequate capacity for applying axial compression loads to the masonry column specimens. The testing setup included the use of five Linear Variable Differential Transformers (LVDTs), with four LVDTs positioned horizontally to measure displacement at each side of the specimen and one LVDT placed vertically to monitor vertical displacement. Loading intervals of 0.25 tons were applied incrementally to the specimens, allowing for controlled loading and accurate data acquisition throughout the test procedure. Figure 5 illustrates the physical arrangement of the specimen test setup in detail. This figure serves to provide visual clarity and aid in understanding the experimental setup employed for conducting the axial compression tests on the masonry column specimens.

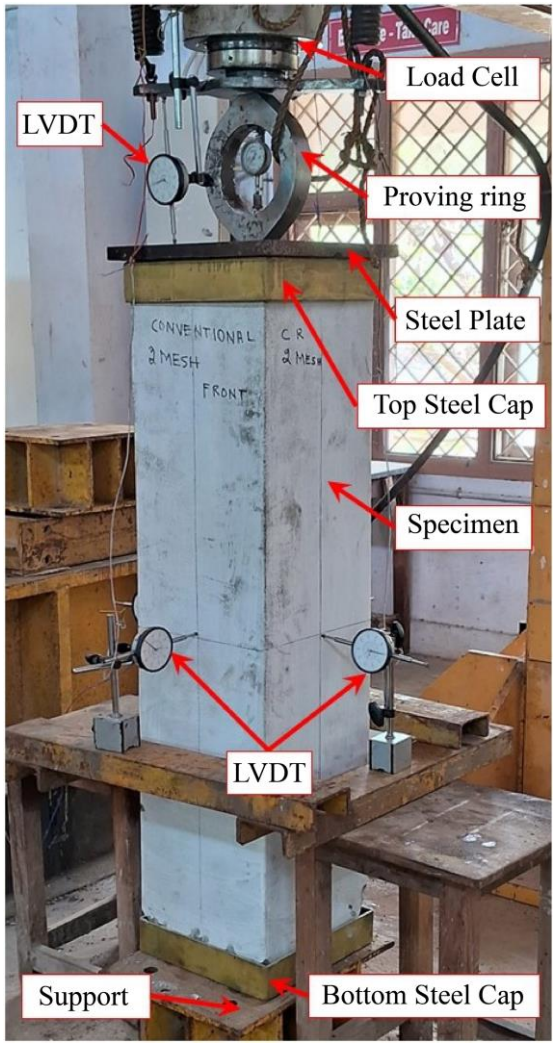

Fig. 5 Test setup

3. Results and Discussion

3.1. Crack Pattern and Failure Mode

Figure 6 shows the crack pattern of the tested specimens, and Figure 7 shows the mode of failure. The observations of the ultimate condition of the tested specimens provide valuable insights into the failure modes and crack patterns exhibited by the masonry columns under axial compression. Specimens UC, CC-0, and GP-0 primarily experienced a brittle vertical crack associated with the crushing of the masonry material (Figure 7a), indicating the inability of the structure to withstand the applied load. Additionally, specimens CC-0, GP-0, GP-1, and GP-2 displayed corner cracks, commonly referred to as the "knife effect," where diagonal cracks originated from the corners of the column, suggesting localized failure and detachment of surface-coated mortar (Figure 7b). Horizontal crack propagation following the initiation of vertical and corner cracks was observed in specimens CC-1, CC-2, GP-1, and GP-2, leading to the detachment of wire mesh reinforcement and surface-coated mortar (Figure 7c), signifying significant structural distress and loss of integrity. Confinement provided by surface-coated mortar and wire mesh reinforcement influenced the failure mechanisms, while the observation of an arching effect (Figure 7d) in specimens CC-2 and GP-2 after the removal of the mortar cap suggested the redistribution of stresses within the column cross-section. Table 5 illustrates the experimental test results.

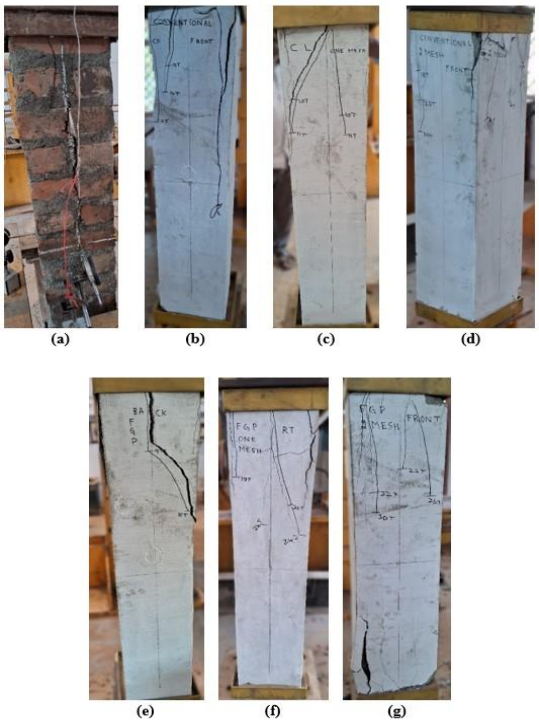

Fig. 6 Crack pattern (a) UC, (b) CC-0, (c) CC-1, (d) CC-2, (e) GP-0, (f) GP-1, and (g) GP-2.

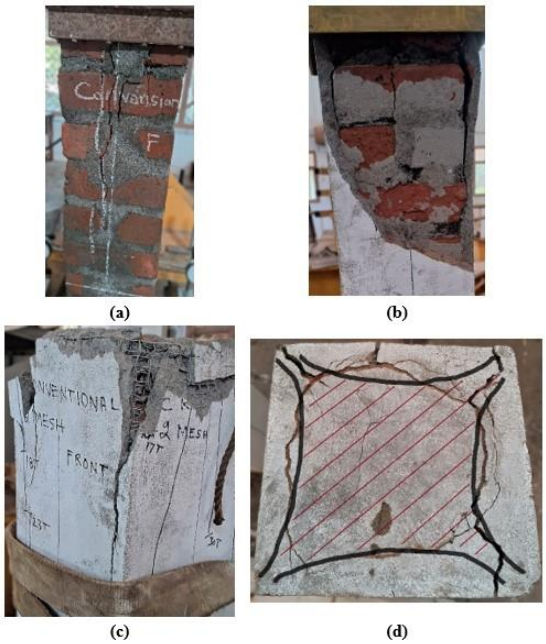

Fig. 7 Mode of failure (a) Crushing of the masonry material, (b) Detachment of surface-coated mortar, (c) Detachment of wire mesh reinforcement and surface-coated mortar, and (d) Arching effect.

3.2. Load Deformation

Figure 8 shows the axial and lateral load-displacement curves of the tested specimens. The results indicate significant variations in vertical and horizontal displacements among the specimens, reflecting differences in structural response to applied loads. Specimens GP-2, GP-1, and CC-2 exhibited the highest vertical displacements, with values of -16.08 mm, -10.35 mm, and -7 mm, respectively. These values correspond to percentage differences of 512.74%, 293.96%, and 166.67%, respectively, compared to the unconfined specimen (UC). The higher percentage variations in vertical displacement for specimens with geopolymer mortar and welded mesh reinforcement suggest enhanced compressibility and deformation capacity, indicative of improved load-bearing capacity and structural resilience. Additionally, specimens GP-1 and GP-2 demonstrated the highest percentage increases in horizontal displacement, particularly on side A, with percentage variations of 557.14% and 208.57%, respectively, compared to UC. These substantial increases in horizontal displacement underscore the enhanced ductility and energy absorption capabilities of specimens incorporating geopolymer mortar and welded mesh reinforcement.

When comparing specimens designated as CC-0 versus GP-0, CC-1 versus GP-1, and CC-2 versus GP-2, noticeable disparities emerge in their structural responses and performance under axial compression. In the comparison between CC-0 and GP-0, both exhibit load capacities of 100 kN and 115 kN, respectively. This represents a 15% increase in load capacity for GP-0. Additionally, GP-0 shows a slightly lower vertical displacement (-2.02 mm) compared to CC-0 (-1.9 mm), resulting in a 6% reduction in vertical deformation and marginally lower horizontal displacement on all sides. Moving to the comparison between CC-1 and GP-1, GP-1 demonstrates a higher load capacity of 200 kN compared to CC-1's 115 kN, reflecting a substantial 74% increase in load capacity for GP-1. However, GP-1 experiences significantly higher vertical displacement (-10.35 mm) compared to CC-1 (-4.95 mm), indicating a 109% increase in vertical deformation, suggesting greater compressibility and higher horizontal displacements.

Similarly, in the comparison between CC-2 and GP-2, GP-2 exhibits a considerably higher load capacity of 370 kN compared to CC-2's 250 kN, demonstrating a significant 48% increase in load capacity for GP-2. Yet, GP-2 also shows significantly higher vertical displacement (-16.08 mm) compared to CC-2 (-7 mm), resulting in a 129% increase in vertical deformation along with higher horizontal displacements. These findings underscore the influence of mortar type and reinforcement strategy on structural behaviour. While geopolymer mortar generally offers higher load capacities, it also exhibits greater deformability compared to cement mortar. This suggests the necessity for meticulous material selection and reinforcement strategies in masonry construction to achieve the desired structural performance and resilience under axial compression.

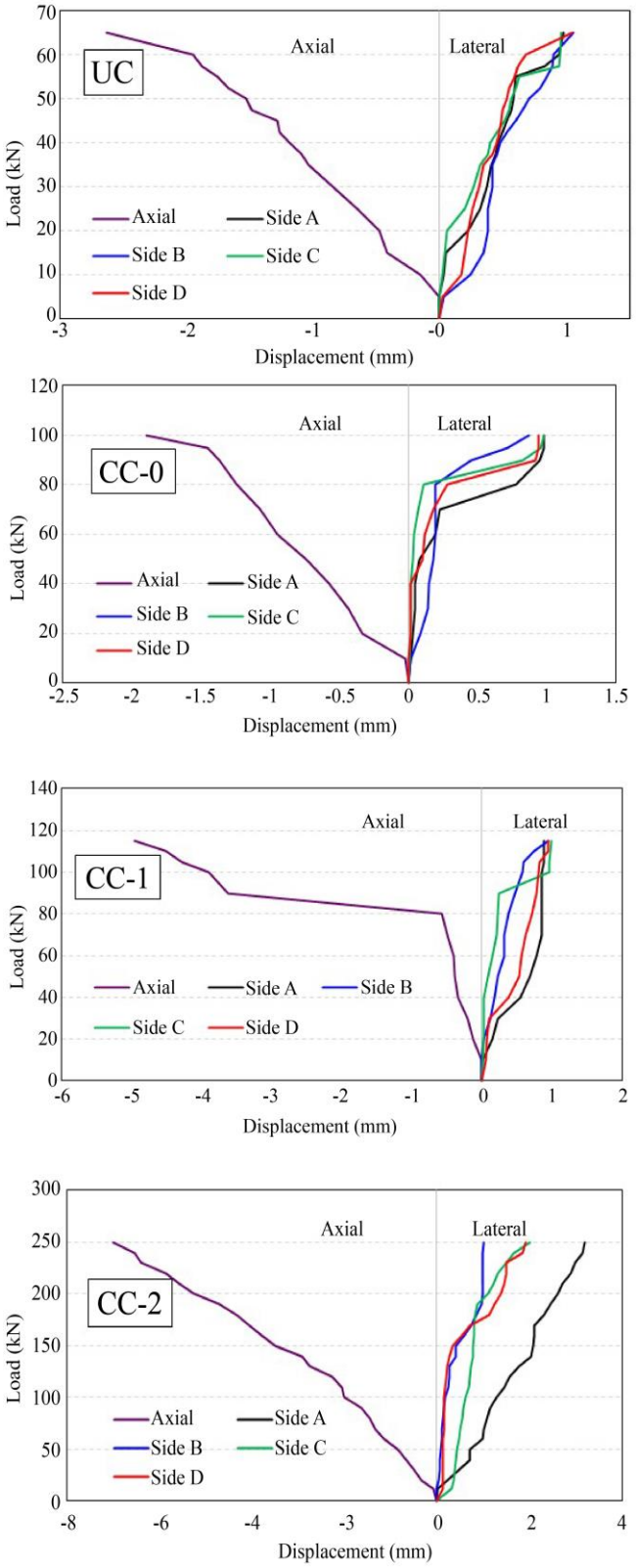

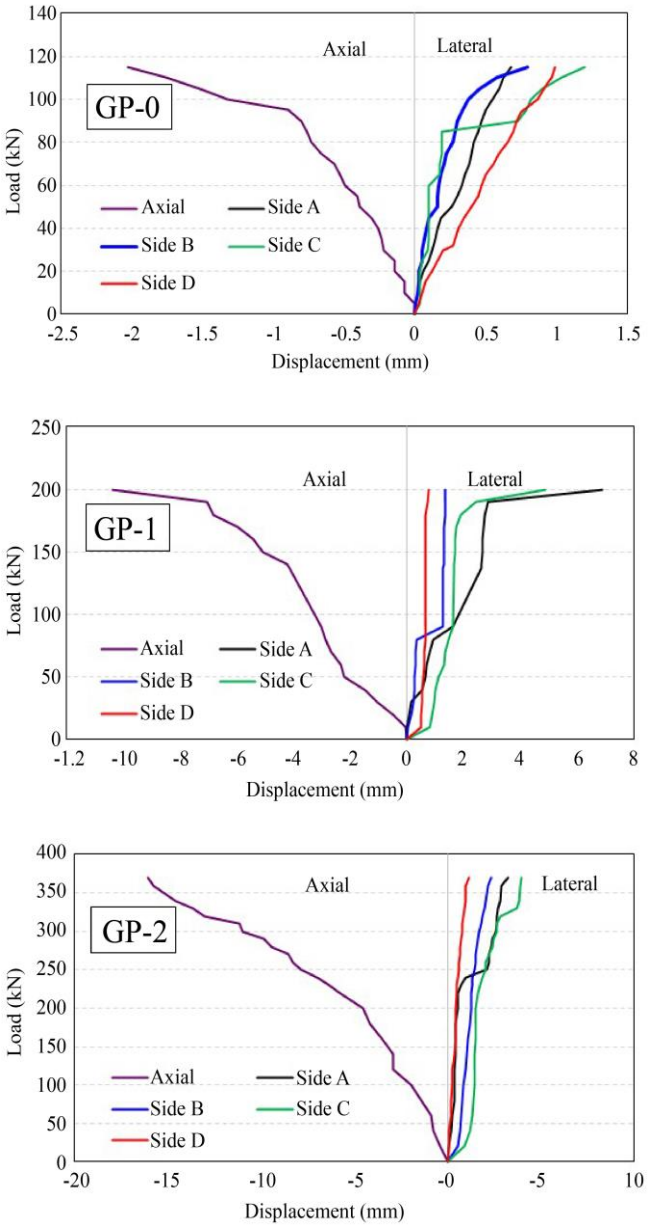

Fig. 8 Axial and lateral load-displacement curves

3.3. Ductility Ratio

Table 5 illustrates the ductility ratios of the tested specimens. Among the specimens, those reinforced with geopolymer mortar (GP-1, GP-2) exhibited notably higher ductility ratios compared to UC, with percentage differences ranging from 11.43% to 49.52%. This indicates a more ductile failure mode characterized by extensive plastic deformation and gradual failure progression due to the presence of welded mesh. At the same time, specimens with lower ductility ratios, like UC, displayed a brittle failure mode with minimal deformation before abrupt failure.

Additionally, the presence of welded mesh reinforcement enhanced the ductility of specimens, as evidenced by the higher ductility ratios observed in CC-1 and CC-2, which demonstrated significant improvements in ductility compared to UC, with percentage differences ranging from 7.62% to 23.81%, attributed to the restrained crack propagation and additional confinement provided by the reinforcement. Furthermore, even specimens without additional reinforcement, such as CC-0 and GP-0, exhibited moderate increases in ductility compared to UC, with percentage differences of 7.62% and 11.43%, respectively. Moreover, differences in geometric configuration, such as multiple layers of welded mesh in CC-2 and GP-2, contributed to variations in ductility ratios, with increased confinement enhancing ductility.

3.4. Energy Absorption

The energy absorption capacities of the tested brick column specimens were investigated, considering the influence of additional confinement materials, mortar types, and reinforcement techniques. The specimens exhibited varying energy absorption values (in kN•mm) displayed in Table 5, with notable differences observed among different configurations. For the unconfined specimen (UC), the energy absorption was measured at 106.76 kN•mm. The percentage difference analysis revealed significant improvements in energy absorption for specimens subjected to confinement and reinforcement.

Table 5. Experimental test results at the ultimate condition

Sample ID	Load (kN)	Axial Displacement (mm)	Lateral Displacement (mm)				Ductility Ratio	Energy Absorption (kN.mm)
			Side A	Side B	Side C	Side D		
UC	65	-2.63	0.98	1.06	0.96	1.05	1.05	106.76
CC-0	100	-1.9	0.98	0.87	0.98	0.94	1.13	114.17
CC-1	115	-4.95	0.88	0.94	0.99	0.95	1.21	422.27
CC-2	250	-7	3.20	1.00	2.00	1.92	1.3	1016.51
GP-0	115	-2.02	0.68	0.80	1.20	0.99	1.17	165.95
GP-1	200	-10.35	6.90	1.30	4.89	0.76	1.26	1368.3
GP-2	370	-16.08	3.24	2.38	4.00	1.15	1.57	3796.45

Table 6. Comparison of experimental results with existing results

Ref.	Specimen	Cross-Section (mm)	Height (mm)	Mesh	Size of Mesh (mm)	No. of Layers	Mortar	Axial Load (kN)	Unconfined / Confined
[49]	Unconfined	225X225	1500	NA	NA	NA	Cement mortar	175	NA
	Confined	270X270	1500	steel wire woven mesh	11.36X11.36	1		400	2.28
[50]	Unconfined	230X230	1500	NA	NA	NA	Cement mortar	233.5	NA
	Confined (Repaired)	270X270	1500	steel wire woven mesh	9.35X9.35	1		491	2.1
						2		525	2.24
	Confined (Retrofitted)					1		495	2.11
						2		545	2.33
[9]	Unconfined	230X230	960	NA	NA	NA	Low strength mortar	247.5	NA
							Medium strength mortar	498.3	
	Confined	230X230	960	Steel Wire	NM	NM	Low strength mortar	327.93	1.32
							Medium strength mortar	585.5	1.74
[51]	Unconfined	215X215	1000	NA	NA	NA	Cement mortar	98.3	NA
	Confined	225X225	1000	0	0	0		120	1.22
				welded steel mesh	19.05X19.05	1 (16 gauge)		190	1.93
						1 (18 gauge)		170	1.72
[52]	Unconfined	250X250	720	NA	NA	NA	Cement mortar	461.25	NA
	Confined	250X250	720	Steel Fiber	0.733X0.733	1	Cement mortar	585	1.26
[53]	Unconfined	240X240	955	0	0	0	Cement mortar	125	NA
	Confined			Steel wire mesh	10X10	1		200	1.6
[11]	Unconfined	250X250	575	NA	NA	NA	Lime based mortar	568	NA
	Confined	250X250	575	Steel Fiber	40X10	1	Lime based mortar	653.75	1.15
						2		716.4	1.28
						3		774.05	1.38
Current study	Unconfined	230X230	1200	NA	NA	NA	Cement mortar	65	NA
	Confined	250X250		0	0	0		100	1.53
		270X270		welded steel mesh	20X20	1		115	1.77
		280X280			20X20	2		250	3.84
		250X250		0	0	0	Geopolymer mortar	115	1.77
		270X270		welded steel mesh	20X20	1		200	3.07
		280X280			20X20	2		370	5.7

NA-Not Applicable; NM- Not Mentioned

Specimens coated with cement mortar (CC-0) and geopolymer mortar (GP-0) exhibited moderate increases in energy absorption, with percentage differences of approximately 6.92% and 55.42%, respectively, compared to the unconfined specimen. However, the presence of welded mesh reinforcement led to substantial enhancements in energy absorption. Single-layer welded mesh reinforcement (CC-1 and GP-1) resulted in dramatic increases in energy absorption, with percentage differences reaching approximately 295.54% and 1181.49%, respectively. Furthermore, double-layer welded mesh reinforcement (CC-2 and GP-2) yielded the highest energy absorption capacities, with percentage differences of approximately 851.03% and 3455.39%, respectively, compared to the unconfined specimen. These findings highlight the significant impact of confinement materials, mortar types, and reinforcement techniques on the energy absorption capabilities of brick column specimens.

Confinement, particularly with welded mesh reinforcement, substantially enhances the structural performance, allowing for greater energy dissipation under axial compression. Moreover, the choice of mortar type, with geopolymer mortar demonstrating superior performance compared to cement mortar, further influenced the energy absorption capacity of the specimens. These findings emphasize the importance of thoughtful material selection and reinforcement strategies in optimizing the resilience and load-bearing capacity of masonry structures. Further investigations are warranted to explore the long-term behaviour and durability of such reinforced masonry systems in practical applications.

4. Comparison of Experimental Results

The current research assesses the effectiveness of geopolymer mortar and mesh layer confinement by comparing it with existing literature. Experimental findings, detailed in Table 1, encompass various parameters such as cross-section, height, mesh type and size, number of layers, mortar composition, and axial load. Additionally, Table 6 presents the ratio of unconfined to confined specimens for each study. A correlation graph (Figure 9) illustrates the relationship between the number of mesh layers and the ratio of unconfined to confined values. The graph indicates that increasing the mesh layer potentially boosts the percentage of axial load, particularly noticeable with geopolymer mortar, where the strength increment surpasses that of conventional mortar. By comparing experimental results between the present and previous studies, the axial load values show a percentage strength increase difference ranging from 15.32% to 469% for the respective tested columns.

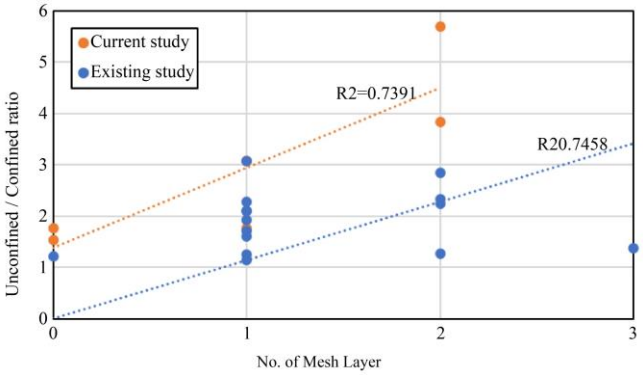

Fig. 9 Correlation between the ratio of unconfined/confined Vs No. of mesh layers

5. Conclusion

Based on the experimental test results, the following conclusion can be drawn:

- Specimens displayed brittle vertical cracks and corner cracks, influenced by surface-coated mortar and wire mesh reinforcement. An arching effect suggested stress redistribution within the column cross-section.
- Significant variations in displacements were observed, with geopolymer mortar and welded mesh reinforcement enhancing compressibility, deformation capacity, and load-bearing capacity compared to unconfined specimens.
- Specimens with geopolymer mortar and welded mesh exhibited higher ductility ratios, indicating a more ductile failure mode. Even specimens without reinforcement displayed moderate increases, emphasizing reinforcement's role in enhancing resilience.
- Energy absorption varied significantly among specimens with welded mesh reinforcement, especially in double-layer configurations, resulting in dramatic increases. Geopolymer mortar demonstrated superior performance in enhancing energy absorption capacities.
- In summary, the study shows that reinforcement strategies and material selection effectively enhance the structural behaviour and load-bearing capacity of masonry columns under axial compression. Geopolymer mortar and welded mesh reinforcement hold promise for improving structural resilience and durability in masonry construction. Further research, including computational modelling like Finite Element Analysis (FEA), is needed to understand and optimize these findings for practical applications fully.

References

[1] Asaad Almssad, Amjad Almusaed, and Raad Z. Homod, "Masonry in the Context of Sustainable Buildings: A Review of the Brick Role in Architecture," *Sustainability*, vol. 14, no. 22, pp. 1-18, 2022. [CrossRef] [Google Scholar] [Publisher Link]

[2] M. Corradi, A. Grazini, and A. Borri, "Confinement of Brick Masonry Columns with CFRP Materials," *Composites Science and Technology*, vol. 67, no. 9, pp. 1772-1783, 2007. [CrossRef] [Google Scholar] [Publisher Link]
[3] Svetlana Brzev, *Earthquake-Resistant Confined Masonry Construction*, pp. 1-81, 2007. [Google Scholar] [Publisher Link]
[4] Sudhir K. Jain et al., "Application of Confined Masonry in a Major Project in India," *NCEE 2014 - 10th U.S. National Conference on Earthquake Engineering Frontiers of Earthquake Engineering*, pp. 1-11, 2014. [Google Scholar]
[5] S.M. Mourad, and M.J. Shannag, "Repair and Strengthening of Reinforced Concrete Square Columns using Ferrocement Jackets," *Cement and Concrete Composites*, vol. 34, no. 2, pp. 288-294, 2012. [CrossRef] [Google Scholar] [Publisher Link]
[6] Luciano Ombres, and Salvatore Verre, "Analysis of the Behavior of FRCM Confined Clay Brick Masonry Columns," *Fibers*, vol. 8, no. 2, pp. 1-19, 2020. [CrossRef] [Google Scholar] [Publisher Link]
[7] Luciano Ombres, and Salvatore Verre, "Masonry Columns Strengthened with Steel Fabric Reinforced Cementitious Matrix (S-FRCM) Jackets: Experimental and Numerical Analysis," *Measurement*, vol. 127, pp. 238-245, 2018. [CrossRef] [Google Scholar] [Publisher Link]
[8] Khalid Saqer Alotaibi, and Khaled Galal, "Axial Compressive Behavior of Grouted Concrete Block Masonry Columns Confined by CFRP Jackets," *Composites Part B: Engineering*, vol. 114, pp. 467-479, 2017. [CrossRef] [Google Scholar] [Publisher Link]
[9] Marinella Fossetti, and Giovanni Minafò, "Strengthening of Masonry Columns with BFRCM or with Steel Wires: An Experimental Study," *Fibers*, vol. 4, no. 2, pp. 1-10, 2016. [CrossRef] [Google Scholar] [Publisher Link]
[10] Jiří Witzany, and Radek Zigler, "Failure Mechanism of Compressed Reinforced and Non-Reinforced Stone Columns," *Materials and Structures*, vol. 48, no. 5, pp. 1603-1613, 2015. [CrossRef] [Google Scholar] [Publisher Link]
[11] Matteo Canestri, Francesca Ferretti, and Claudio Mazzotti, "Confinement of Masonry Columns through SRG: Experimental Results and Analytical Prediction," *Procedia Structural Integrity*, vol. 44, pp. 2198-2205, 2022. [CrossRef] [Google Scholar] [Publisher Link]
[12] Habib Allah Poornamazian, and Mohsen Izadinia, "Prediction of Compressive Strength of Brick Columns Confined with FRP, FRCM, and SRG System using GEP and ANN Methods," *Journal of Engineering Research*, pp. 1-14, 2023. [CrossRef] [Google Scholar] [Publisher Link]
[13] Mohana Rajendran, "Corrosion Assessment of Ferrocement Element with Nanogeopolymer for Marine Application," *Structural Concrete Journal of the Fib*, vol. 22, no. 5, pp. 2882-2894, 2021. [CrossRef] [Google Scholar] [Publisher Link]
[14] Taha Awadallah El-Sayed, "Axial Compression Behavior of Ferrocement Geopolymer HSC Columns," *Polymers*, vol. 13, no. 21, pp. 1-31, 2021. [CrossRef] [Google Scholar] [Publisher Link]
[15] J. Revathy, P. Gajalakshmi, and M. Aseem Ahmed, "Flowable Nano SiO_2 based Cementitious Mortar for Ferrocement Jacketed Column," *Materials Today Proceedings*, vol. 22, pp. 836-842, 2020. [CrossRef] [Google Scholar] [Publisher Link]
[16] Mohana Rajendran, and Nagan Soundarapandian, "Geopolymer Ferrocement Panels under Flexural Loading," *Science and Engineering of Composite Materials*, vol. 22, no. 3, pp. 331-341, 2015. [CrossRef] [Google Scholar] [Publisher Link]
[17] S.S. Arun Kumar, A. Madhavan, and S. Dharmar, "Experimental Srudy on Impact Resistance of Geopolymer Ferrocement Flat Panel," *International Conference on Recent Trends in Civil Engineering, Technology and Management*, pp. 278–282, 2017. [Google Scholar] [Publisher Link]
[18] Joseph Davidovits, "Geopolymer Cement A Review," *Geopolymer Science and Technics*, pp. 1-11, 2013. [Google Scholar] [Publisher Link]
[19] Joseph Davidovits, "Properties of Geopolymer Cements," *Proceedings First International Conference on Alkaline Cements and Concretes*, pp. 131-149, 1994. [Google Scholar] [Publisher Link]
[20] Joseph Davidovits, "Geopolymer Chemistry and Sustainable Development. The Poly (Silicate) Terminology: A Very Useful and Simple Model for the Promotion and Understanding of Green-Chemistry," *Geopolymer 2005 Conference*, Saint-Quentin, France, pp. 9-16, 2005. [Google Scholar]
[21] Djwantoro Hardjito, and B. Vijaya Rangan, "*Development and Properties of Low-calcium Fly Ash Based Geopolymer Low-Calcium Fly Ash-Based Geopolymer Concrete*," Curtin University of Technology, pp. 1-103, 2005. [Google Scholar] [Publisher Link]
[22] Chakradhara R. Meesala, Nikhil K. Verma, and Shailendra Kumar, "Critical Review on Fly-Ash Based Geopolymer Concrete," *Structural Concrete Journal of the Fib*, vol. 21, no. 3, pp. 1013-1028, 2020. [CrossRef] [Google Scholar] [Publisher Link]
[23] C. Prithiviraj, and J. Saravanan, "Flexural Performance of Alccofine-based Self-Compacting Concrete Reinforced with Steel and GFRP Bars," *International Transaction Journal of Engineering, Management, & Applied Sciences & Technologies*, vol. 12, no. 8, pp. 1-12, 2021. [CrossRef] [Google Scholar] [Publisher Link]
[24] Chidambaram Prithiviraj et al., "Fresh and Hardened Properties of Self-Compacting Concrete Comprising a Copper Slag," *Buildings*, vol. 12, no. 7, pp. 1-21, 2022. [CrossRef] [Google Scholar] [Publisher Link]
[25] Prithiviraj Chidambaram, and Saravanan Jagadeesan, "Characteristics of Self-Compacting Concrete with Different Size of Coarse Aggregates and Alccofine," *Trends in Sciences*, vol. 19, no. 5, pp. 1-17, 2022. [CrossRef] [Google Scholar] [Publisher Link]
[26] Chidambaram Prithiviraj et al., "Assessment of Strength and Durability Properties of Self-Compacting Concrete Comprising Alccofine," *Sustainability*, vol. 14, no. 10, pp. 1-19, 2022. [CrossRef] [Google Scholar] [Publisher Link]

[27] Wu Chen, and Zhiduo Zhu, "Utilization of Fly Ash to Enhance Ground Waste Concrete-Based Geopolymer," *Advances in Materials Science and Engineering*, vol. 2018, pp. 1-11, 2018. [CrossRef] [Google Scholar] [Publisher Link]

[28] B.G. Vishnuram et al., "Fly-Ash and GGBS Based Geo-Polymer Concrete with Granite Powder as Partial Replacement of M-Sand for Sustainability," *Materials Today Proceedings*, 2023. [CrossRef] [Google Scholar] [Publisher Link]

[29] Gaurav Jagad, C.D. Modhera, and Dhaval Patel, "Experimental Investigation on Development of Compressive Strength of High-Strength Geopolymer Concrete Containing M-Sand," *Sustainable Building Materials and Construction*, pp. 21-29, 2022. [CrossRef] [Google Scholar] [Publisher Link]

[30] A. Chithambar Ganesh et al., "Durability Studies on the Hybrid Fiber Reinforced Geopolymer Concrete Made of M-Sand Under Ambient Curing," *IOP Conference Series: Materials Science and Engineering*, vol. 981, pp. 1-11, 2020. [CrossRef] [Google Scholar] [Publisher Link]

[31] V. Sreevidya, R. Anuradha, and R. Venkatasubramani, "Experimental Study on Geopolymer Ferro Cement Slab using Various Wire Meshes," *Journal of Structural Engineering*, vol. 39, no. 4, pp. 436-443, 2012. [Google Scholar]

[32] V. Sreevidya et al., "Flexural Behavior of Geopolymer Ferrocement Elements," *Asian Journal of Civil Engineering*, vol. 15, no. 4, pp. 563-574, 2014. [Google Scholar] [Publisher Link]

[33] S. Kaliraj, P. Madasamy, and S. Dharmar, "Impact Behaviour of Geopolymer Ferrocement Trough Panel," *International Conference on Recent Trends in Civil Engineering, Technology and Management*, pp. 496–500, 2017. [Google Scholar] [Publisher Link]

[34] T. Chaitanya Srikrishna, and T.D. Gunneswara Rao, "A Study on Flexural Behavior of Geopolymer Mortar Based Ferrocement," *Materials Today Proceedings*, vol. 43, pp. 1503-1512, 2020. [CrossRef] [Google Scholar] [Publisher Link]

[35] Dharmar Sakkarai, and Nagan Soundarapandian, "Strength Behavior of Flat and Folded Fly Ash-Based Geopolymer Ferrocement Panels under Flexure and Impact," *Advances in Civil Engineering*, vol. 2021, pp. 1-13, 2021. [CrossRef] [Google Scholar] [Publisher Link]

[36] T. Kibriya, "A Study on Use of Blended Ferrocement: A High Performance Material for Repair/Strengthening of Brick Masonry Columns," *WIT Transactions on the Built Environment*, vol. 85, pp. 469-478, 2006. [CrossRef] [Google Scholar] [Publisher Link]

[37] Abid A. Shah, "Applications of Ferrocement in Strengthening of Unreinforced Masonry Columns," *International Journal of Geology*, vol. 5, no. 1, pp. 21-27, 2011. [Google Scholar] [Publisher Link]

[38] Marinella Fossetti, and Giovanni Minafò, "Strengthening of Masonry Columns with BFRCM or with Steel Wires: An Experimental Study," *Fibers*, vol. 4, no. 2, pp. 1-10, 2016. [CrossRef] [Google Scholar] [Publisher Link]

[39] Enea Mustafaraj, and Yavuz Yardım, "Usage of Ferrocement Jacketing for Strengthening of Damaged Unreinforced Masonry (URM) Walls," *3rd International Balkans Conference on Challenges of Civil Engineering*, pp. 19-21, 2016. [Google Scholar] [Publisher Link]

[40] Debasish Sen et al., "Lateral Strength Evaluation of Ferrocement Strengthened Masonry Infilled RC Frame Based on Experimentally Observed Failure Mechanisms," *Structures*, vol. 58, 2023. [CrossRef] [Google Scholar] [Publisher Link]

[41] IS: 12269-1987, Specification for 53 Grade Ordinary Portland Cement, Bureau of Indian Standards, pp. 1-17, 2013. [Online]. Available: https://law.resource.org/pub/in/bis/S03/is.12269.1987.pdf

[42] IS: 383-2016, Specification for Coarse and Fine Aggregates from Natural Sources for Concrete, Bureau of Indian Standards, pp. 1–21, 2016. [Online]. Available: http://icikbc.org/docs/IS383-2016.pdf

[43] IS: 9103-2018, Concrete Admixtures-Specification, Bureau of Indian Standards, pp. 1-17, 2018. [Online]. Available: https://pdfcoffee.com/9103-reaffirmed-2018pdf-pdf-free.html

[44] R. Anu, and S. Thirugnanasambandam, "Development of Ambient Cured Geopolymer Bricks," *International Journal Advanced Research Engineering and Technology*, vol. 12, no. 2, pp. 229–236, 2021. [CrossRef] [Google Scholar] [Publisher Link]

[45] S. Thirugnanasambandam, "*Development of Geopolymer Concrete and Testing of Elements*," Chidambaram, Annamalai Nagar, 2018. [Publisher Link]

[46] IS: 4031 (Part 6) - 1988, Methods of Physical Tests for Hydraulic Cement, Bureau of Indian Standards, pp. 1-11, 1988. [Online]. Available: https://ia600306.us.archive.org/35/items/gov.in.is.4031.6.1988/is.4031.6.1988.pdf

[47] IS 1077: 1992, Common Burnt Clay Building Bricks- Specifications, Bureau of Indian Standards, pp. 1-10, 1992. [Online]. Available: https://law.resource.org/pub/in/bis/S03/is.1077.1992.pdf

[48] ASTM A185-79, Standard Specification for Welded Steel Wire Fabric for Concrete Reinforcement, ASTM International, 1979. [Online]. Available: https://www.astm.org/a0185-79.html

[49] Ambhore Vinavak Parashram, "*Behaviour of Ferrocement Encased Brick Masonry Columns*," Department of Civil Engineering University of Roorkee, pp. 1-69, 2000. [Publisher Link]

[50] Amit Garg, "*Ferrocement Applications in Repair and Retrofitting of Brick Masonry Columns*," Department of Civil Engineering Indian Institute of Technology Roorkee, pp. 1-73, 2004. [Publisher Link]

[51] Geeta Mehta, N.P. Devgan, and Amit Mehta, "Modified Failure Load for Brick Masonry Columns Encased with Ferrocement - An Experimental Study," *International Journal of Earth Sciences and Engineering*, vol. 10, no. 2, pp. 321-325, 2017. [Google Scholar] [Publisher Link]

[52] Lesley H. Sneed et al., "Confinement of Clay Masonry Columns with SRG," *Key Engineering Materials*, vol. 747, pp. 350–357, 2017. [CrossRef] [Google Scholar] [Publisher Link]

[53] M.Q. Adnan et al., "Performance of Solid Masonry Columns After Strengthening," *Journal of Physics Conference Series*, vol. 1973, no. 1, pp. 1-8, 2021. [CrossRef] [Google Scholar] [Publisher Link]